

УДК 539.172.12

**VARIATION OF THE COULOMB REPULSION
IN MULTIFRAGMENTATION**

*H. Oeschler*¹, *A.S. Botvina*², *D.H.E. Gross*³, *S.P. Avdeyev*⁴,
*V.A. Karnaukhov*⁴, *L.A. Petrov*⁴, *V.K. Rodionov*⁴, *O.V. Bochkarev*⁵,
*L.V. Chulkov*⁵, *E.A. Kuzmin*⁵, *A. Budzanowski*⁶, *W. Karcz*⁶, *M. Janicki*⁶,
*E. Norbeck*⁷

In multifragment emission, the measured Coulomb repulsion provides evidence for the initial geometry and the time evolution of the break-up process. In collisions of light relativistic projectiles with gold, it is found that for a given isotope the maxima of the energy spectra decrease with increasing number of emitted fragments. This could indicate a variation in density at break-up. Different explanations of this observation are considered. Statistical multifragmentation models with fixed density provide a similar effect.

The investigation has been performed at the Dzhelapov Laboratory of Nuclear Problems, JINR.

**Вариации кулоновского взаимодействия
при мультифрагментации**

Х.Ойшлер и др.

При эмиссии фрагментов промежуточной массы кулоновское расталкивание дает информацию об исходной геометрии и эволюции во времени процесса развала системы. Во взаимодействиях релятивистских частиц с золотом обнаружено, что для данного изотопа максимум энергетического спектра смещается в сторону меньших энергий с увеличением числа вылетевших фрагментов. Это может быть проявлением изменения плотности системы. Рассматриваются различные объяснения этого феномена. Статистические модели мультифрагментации с фиксированной плотностью дают сходный эффект.

Работа выполнена в Лаборатории ядерных проблем им. В.П.Джелепова ОИЯИ.

¹Institut für Kernphysik, Technische Universität Darmstadt, D-64289 Darmstadt, Germany

²INFN and Dipartimento di Fisica, 40126 Bologna, Italy

³Hahn-Meitner-Institut, Bereich Theorie, D-14109 Berlin, Germany

⁴Joint Institute for Nuclear Research, 141980, Dubna, Russia

⁵Kurchatov Institute, 123182, Moscow, Russia

⁶H.Niewodniczanski Institute for Nuclear Physics, 31-342, Cracow, Poland

⁷University of Iowa, Iowa City, IA 52242, USA

1. INTRODUCTION

The understanding of the emission of intermediate mass fragments (IMF) from highly excited nuclei is a major topic in current nuclear physics research. This process gives access to the behaviour of nuclear matter at low densities and nuclear phase transitions.

To understand this new decay mechanism detailed knowledge of the excitation energy, of the density at break-up and of the time scales involved are of key interest. The study of the repulsive Coulomb forces between the emitted fragments gives information about the situation at break-up, e.g., on density and on the time scale of emission using velocity and angular correlations [1–9].

This work is focused on the detailed study of the energy spectra of the emitted fragments. For thermal multifragmentation the kinetic energy of the fragments is mainly determined by Coulomb interactions. The maxima of the spectra are generally at rather low energies which could imply a dilute configuration at break-up. A reduced Coulomb repulsion was observed already in 1964 by Cumming et al. [10] and later reported in several papers [11]. A more detailed study reveals that the shape of the spectra varies with the number of emitted fragments as demonstrated in this work: the larger the number of fragments, the lower the maximum of the energy spectra. A similar observation has been reported in Ref. 12 and it was interpreted as a reduction of the density when more fragments are emitted. In addition to our experimental finding a detailed analysis of model calculations will be discussed in view of alternative explanations of this variation.

2. EXPERIMENTAL SET-UP

The study is based on experimental results on p + Au collision at 8.1 GeV incident energy (at several GeV incident energy). These experiments were performed at the synchrophasotron in Dubna, Russia, using the modified [13] 4π -set-up FASA [14]. A survey of the results using protons at incident energies of 2.1, 3.6, and 8.1 GeV are given in Ref. 15.

The device consists of five ΔE (ionisation chambers) \times E (Si)-telescopes, and 64 CsI(Tl) counters as fragment multiplicity detectors (FMD). The ionisation chambers are located at angles from 24° to 156° and cover a solid angle of 0.03 sr. They serve as the trigger for the read-out of the system. The FMD cover 89% of 4π and gives the number of IMF's in an event. A self-supporting Au target 1.5 mg/cm^2 thick was located in the centre of the FASA vacuum chamber. The average beam intensity was $7 \cdot 10^8$ p/spill for protons and α beams and $1 \cdot 10^8$ p/spill for carbon projectiles with a spill length of 300 ms and a spill period of 10 s.

3. EXPERIMENTAL RESULTS

The experimental observation to be discussed here is the variation of the energy spectra with IMF multiplicity. This has been observed in collisions of p with Au at 8.1 GeV incident energy and all outgoing isotopes exhibit the same trend. Figure 1 displays typical examples of energy spectra selected according to the measured IMF multiplicity M_A . It shows various ejectiles measured in p + Au at 8.1 GeV. We denote M_A as the IMF multiplicity measured by

the multiplicity array (FMD) without counting the triggering IMF. Hence, the measured total IMF multiplicity (of events with at least one IMF) is $1 + M_A$. As the detection efficiency is less than 100%, the energy spectra for a given M_A are mixtures of contributions from different primary multiplicities with weights as given in Eq. (1) of Ref. 15.

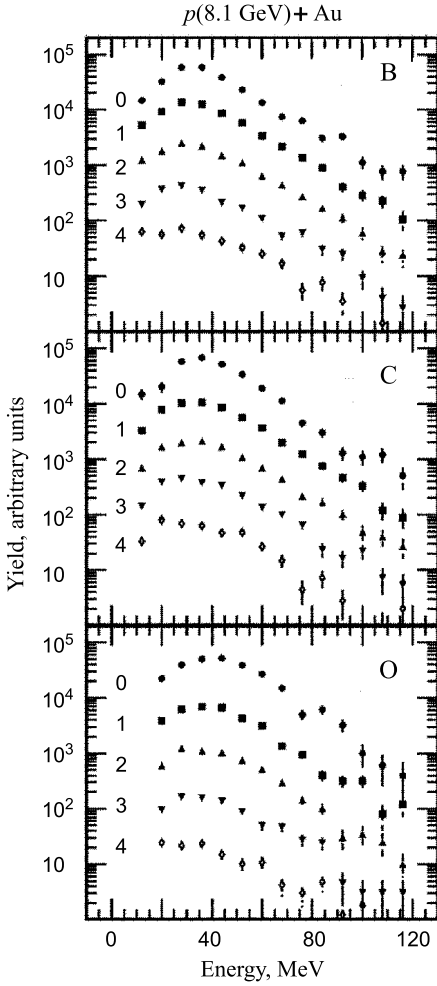


Fig. 1. Examples of the variation of energy spectra of B, C, and O with IMF multiplicity. M_A gives the measured number of IMF's in addition to the detected isotope

ing the dynamics of the self-consistent nuclear field, the INC is rather successful in describing the distributions of RN for peripheral collisions and for reactions of small projectiles with heavy nuclei.

At high excitation energy the main de-excitation mechanism of RN is their break-up into many large particles — multifragmentation [20]. In the present work, for simulating nuclear

For all examples typical trends are seen: (i) the inverse slope parameters at high kinetic energies increase with increasing M_A ; (ii) the energies of the maxima of the spectra decrease with M_A . While the slope variation likely reflects the selection of different excitation energies, E_x , (the more IMF's, the higher E_x), the second point deserves a careful study by performing model calculations.

4. CALCULATIONS

Such complicated nuclear reactions are commonly considered as multistage processes. The simplest way is to divide the reaction into two stages: nonequilibrium and equilibrium. The reason for this is the sharp difference of time scale and character of processes taking place during these stages.

The intranuclear cascade model (INC) is widely used for simulating the initial nonequilibrium stage of nucleus-nucleus reactions [16–18]. The physical picture of the INC is simple: the incident nucleus initiates cascades of successive quasi-free nucleon-nucleon and pion-nucleon collisions. High-energy products of the hadron-nucleon collisions leave the nuclei while low-energy particles are trapped by them. After completion of the cascades, the residues of the nuclei are characterized by the number of nucleons A , of protons Z , by their excitation energy E_x , by their momentum \vec{P} , and angular momentum \vec{L} . Usually these residual nuclei (RN) are identified with equilibrated systems. However, an additional preequilibrium emission may be important for the total thermalization of RN [19] or an expansion leading to densities at which break-up occurs [15]. In spite of disregarding

disintegration we use two multifragmentation models: Microcanonical Metropolis Monte Carlo model (MMMC) [21–23] and the statistical multifragmentation model (SMM) [20, 24]. For a comparison of these two approaches see Ref. 25.

Within MMMC and SMM we consider a microcanonical ensemble of all break-up channels composed of nucleons and excited fragments of different masses. It is assumed that an excited nucleus expands and the decoupling of the fragments (freeze-out) occurs at a certain volume V . Fragments may be created earlier, yet, they still interact. At freeze-out the system is supposed to be in statistical equilibrium and the probability W_j of a decay channel j is proportional to its statistical weight

$$W_j \sim \exp S_j(E_x, A, Z, \vec{P}, \vec{L}, V), \quad (1)$$

where S_j is the entropy of the system in a state corresponding to the decay channel j . After the freeze-out (last strong interaction) the fragments propagate independently in their mutual Coulomb fields and might undergo secondary decays. The models differ by sampling channels in this ensemble: the Metropolis method used in MMMC and the direct random generation used in SMM and also, by details in the de-excitation of hot fragments and their Coulomb interaction. The MMMC calculates Coulomb energy by taking the real positions of fragments inside the volume, the SMM finds the mean Coulomb energy in the Wigner–Seitz approximation. The MMMC considers the secondary de-excitation as fast emission of nucleons at the location where the fragment is formed, the SMM takes into account evaporation of all light particles (including fission for heavy fragments) but after the Coulomb acceleration. For many observed characteristics (e.g., yield and multiplicity of fragments) these differences are not essential and both models give similar results.

These two models are applied for simplicity to the decay of $A = 160$ nuclei at excitation energies of 4, 5, and 6 MeV/nucleon. These values are guided by the INC calculation performed for the system p+Au at 8.1 GeV. The choice of a constant A and fixed E_x is made to show properties of the model calculations in a transparent way. Realistic calculations would, of course, require distributions in A , charge and E_x . Fixed decoupling densities of $\rho/\rho_0 = 1/6$ (MMMC) and $1/3$ (SMM) are used*. The choice of the densities does not influence the trends discussed here, of course higher mean energies are obtained for more compact break-up conditions.

5. DISCUSSIONS

Of interest is the change of the mean values and the maxima of the energy distributions with IMF multiplicity. This is demonstrated in Fig. 2 for outgoing carbon isotopes. The upper part shows the trend of the mean energy and the energy with maximum yield with $M_A + 1$ as deduced from the measured spectra for p+Au collisions. The middle and lower parts of Fig. 2 show the calculated $\langle E \rangle$ as a function of the primary IMF multiplicity. The scaling of the two abscissas are chosen such that their mean values correspond to each other. It is interesting to note that the calculations show a decrease even when both excitation energy

*As described in [24] SMM uses a parametrized multiplicity-dependent volume for calculating phase-space probabilities of partitions but the calculation of Coulomb and kinetic energies of fragments is made in a fixed volume that is three times larger than the normal one.

and density are fixed. Therefore, the observation of a drop does not imply a change in the density as the application of the Coulomb law intuitively suggests. This decrease is inherent in the multifragment-decay process.

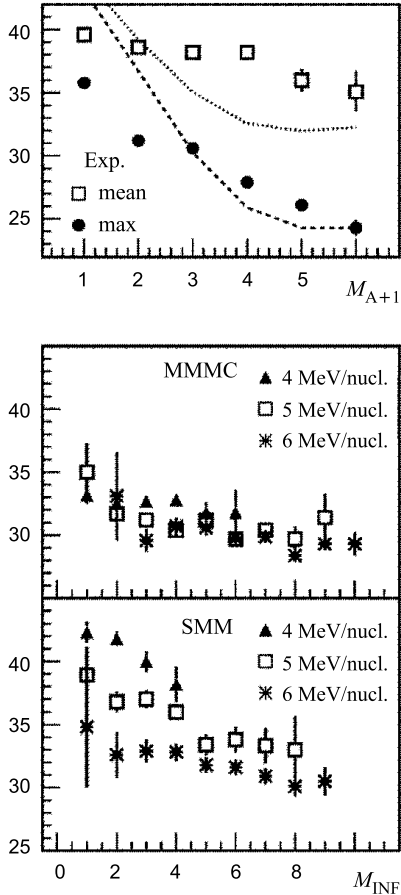


Fig. 2. Mean energy (and E_{\max}) of outgoing carbon isotopes as a function of the IMF multiplicity for p+Au collisions. The upper part gives the experimental results (symbols) deduced from the spectra shown in Fig.1. The lines exhibit the results of an INC+Expansion+SMM calculation for E_{\max} (dashed) and $\langle E \rangle$ (dotted), folded with the experimental filter (see text). The middle and lower part shows the results of the MMMC and SMM calculations of decaying $A=160$ nuclei at fixed excitation energies with values as indicated

Before discussing the origin of the change of fragment energies with multiplicity, differences between MMMC and SMM should be mentioned. Figure 2 shows that in the SMM model $\langle E \rangle$ varies with excitation energy while in the MMMC calculations such a trend is very weak, practically not visible. This arises probably from the different number of charged particles taking part in the acceleration process in the two models. The SMM model considers acceleration of a few hot fragments. Protons and α particles are produced mainly long after freeze-out as a result of secondary de-excitation and this emission influences considerably the energies of IMF's. In MMMC protons and α particles participate in the acceleration on an equal footing with the cold fragments. The nuclear system is initially disintegrated into many more particles and their energies change slowly with an increasing number of emitted particles. This is seen in Fig.3: in the freeze-out volume the fragment charges are considerably larger for the SMM case (top); the relative share of the total kinetic energy obtained by carbon in SMM depends strongly on the number of IMF's while in the MMMC case it depends much less on the surrounding IMF's (bottom). Therefore, the difference between the two models might be used to experimentally determine the importance and the instant of secondary decay of fragments during their Coulomb acceleration.

Detailed calculations of carbon energy spectra have been performed with SMM. The input data (charge, mass and excitation energies of fragmenting nuclei) are taken from INC calculations taking into account the loss of mass and excitation energy during the expansion stage as suggested in Ref. 15. As the remnant nuclei after INC are close to normal nuclear matter density but SMM starts with low density, the direct combination of the two models is inconsistent. In [15] the expansion is taken into account rather empirically by fitting the measured IMF multiplicities. It should be stated that in the studied reactions the expansion stage influences little the energy spectra, as they are mainly governed by the density used in the SMM model.

The calculated energy spectra are folded with the experimental filter according to Eq.(1) in Ref. 15. These calculations render well the inclusive carbon spectrum (see Ref. 15). As the excitation energy of the fragmenting system varies from ≈ 2 to ≈ 6 MeV/nucleon (with a mean value of ≈ 4 MeV/nucleon [15]), this model gives a rather strong decrease of E_{max} and $\langle E \rangle$ for carbon spectra with multiplicity (dotted and dashed lines in the upper part of Fig. 2) which is stronger than the measured trend. In contrast, the MMMC model predicts that $\langle E \rangle$ hardly changes with excitation energy (Fig. 2, middle part). Hence, the discrepancy between the measured trend and the SMM prediction might indicate that the de-excitation of hot fragments proceeds mainly during or, similar to the MMMC case, in the beginning of the Coulomb acceleration.

One might think that the carbon isotopes are emitted more at the surface when only few fragments are present and, in the other case, with many fragments simultaneously, the emission might occur more in the centre. In our model calculations we can trace back the origin of the fragments. As shown in the middle part of Fig. 3, the mean relative distance from the center of mass does hardly vary with the number of fragments.

The observed effect appears as a consequence of many-body Coulomb evolution for partitions.

It should be mentioned that sequential fragment emission also yields the observed trend. With the sequential binary model [26] the later the carbon is emitted, the lower its kinetic energy. This is due to the decreasing charge and excitation energy of the system with time. However, the time scale in this model is significantly larger than the time estimated experimentally [7].

6. SUMMARY

The energy spectra of outgoing fragments in multifragmentation reactions exhibit a decreasing «Coulomb peak» as the IMF multiplicity increases. Performing calculations with statistical multifragmentation models we conclude that a drop in E_{max} and $\langle E \rangle$ of the outgoing fragments with increasing IMF multiplicity alone is not a proof for a varying density nor of a different emission geometry. Such a trend is consistent with the Coulomb interaction of many-particle systems in general. The observed variation of

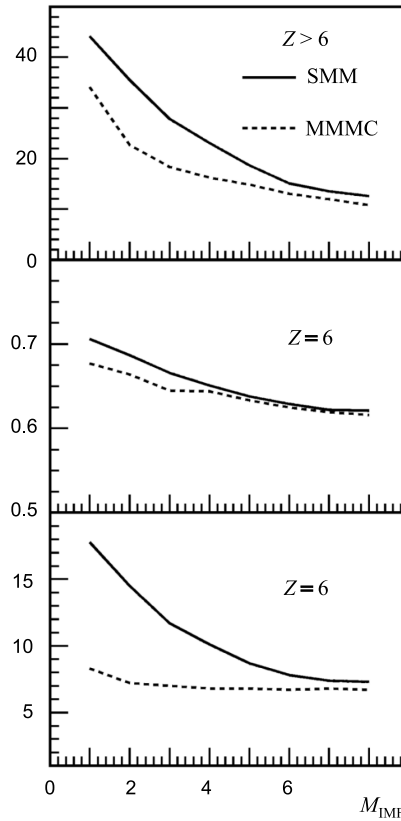


Fig. 3. MMMC and SMM calculations for the multifragmentation of ^{160}Gd nuclei at excitation energy 5 MeV/nucleon. The SMM results are for hot fragments leading after secondary de-excitation to a carbon (middle and bottom) and to fragments with $Z > 6$ (top). Top: average charge for fragments with $Z > 6$; middle: relative distance of fragments with $Z = 6$ from the centre mass of the system (note the suppressed origin); bottom: relative share of the total kinetic energy of fragments with $Z=6$ after the Coulomb acceleration

the energy spectra has a natural explanation in the kinematical redistribution of the energy with increasing disintegration of the system as predicted by statistical models. It is clear from the comparison of the models that in future experimental studies the analysis of fragment-energy distributions at different fragment multiplicities can provide crucial information about the internal excitation of the fragments and their Coulomb interaction and propagation during secondary de-excitation.

The authors are thankful to Prof. A.Hryniewicz, A.M.Baldin, S.T.Belyaev, A.I.Malakhov, and N.A.Russakovich for support. The research was supported in part by Grant No. 00-02-16608 from Russian Foundations for Basic Research, by Grant No. 94-2249 from INTAS, by Grant from Polish Plenipotentiary of JINR, by Grant No. 2P03 12615 from the Polish State Committee for Scientific Research, by Contract No. 06DA819 from the German Bundesministerium für Bildung und Wissenschaft and by the US National Science Foundation.

References

1. Trockel R. et al. — Phys. Rev. Lett., 1987, v.59, p.2844.
2. Bougault R. et al. — Phys. Lett. B, 1989, v.232, p.291.
3. Kim Y.D. et al. — Phys. Rev. Lett., 1991, v.67, p.14; Phys. Rev. C, 1992, v.45, p.387; Bowman D.R. et al. — *ibid.*, 1995, v.52, p.818.
4. Fox D. et al. — Phys. Rev. C, 1993, v.47, p.R421.
5. Kämpfer B. et al. — Phys. Rev. C, 1993, v.48, p.R955.
6. Bao-An Li, Gross D.H.E., Lips V., Oeschler H. — Phys. Lett. B, 1994, v.335, p.1.
7. Lips V. et al. — Phys. Lett. B, 1994, 338, p.141; Shmakov S.Y. et al. — Yad. Fiz., 1995, v.58, p.1735; (Phys. of Atomic Nucl., 1995, v.58, p.1635).
8. Gelderloos C., Alexander J.M. — Nucl. Instrum. Methods Phys. Res. A, 1994, v.349, p.618; Gelderloos C. et al. — Phys. Rev. Lett., 1995, v.75, p.3082.
9. Wang G. et al. — Phys. Rev. C, 1998, v.57, p.R2786.
10. Cumming J.B. et al. — Phys. Rev. B, 1964, v.167, p.134.
11. Milkau U. et al. — Phys. Rev. C, 1991, v.44, p.R1242.
12. K. Kwiatkowski et al. — Phys. Rev. Lett., 1995, v.74, p.3756; Foxford E.R. et al. — Phys. Rev. C, 1996, v.54, p.749.
13. Avdeyev S.P. et al. — Pribory i Tekhnika Eksper., 1996, .39, p.7; (Instr. Exp. Techn. 39 (1996) 153).
14. Avdeyev S.P. et al. — Nucl. Instr. and Meth. A, 1993, v.332, p.149.

15. Avdeyev S.P. et al. — *Eur. Phys. J. A*, 1998, v.3, p.75.
16. Fraenkel Z. et al. — *Phys. Rev. C*, 1982, v.26, p.1618.
17. Cugnon J., Kinet D., Vandermeulen J. — *Nucl. Phys.*, 1982, v.A379, p.553.
18. Toneev V.D., Gudima K.K. — *Nucl. Phys. A*, 1983, v.400, p.173c.
19. Botvina A.S., Mishustin I.N. — *Phys. Lett. B*, 1992, v.294, p.23.
20. Botvina A.S. et al. — *JETP Lett.* , 1985, v.42, p.572;
Botvina A.S., Iljinov A.S., Mishustin I.N. — *Nucl. Phys. A*, 1990, v.507, p.649.
21. Zhang X., Gross D.H.E., Xu S., Zheng Y. — *Nucl. Phys. A*, 1987, v.461, p.641.
22. Gross D.H.E. — *Rep. Progr. Phys.*, 1990, 53, p.605.
23. Gross D.H.E. — *Physics Report*, 1997, v.279, p.119.
24. Botvina A.S. et al. — *Nucl. Phys. A*, 1987, 475, p.663;
Bondorf J., A.S. Botvina A.S., Iljinov A.S., Mishustin I.N., Sneppen K. — *Physics Report*, 1995, v.257, p.133.
25. Gross D.H.E., Sneppen K. — *Nucl. Phys. A*, 1994, v.567, p.317.
26. Wagner P. et al. — *Phys. Lett. B*, 1999, v.460, p.31.

Received on April 25, 2000.